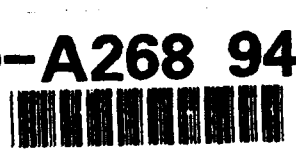

PL-TR-93-2150

UPPER ATMOSPHERIC EFFECTS OF THE HF ACTIVE AURORAL RESEARCH PROGRAM IONOSPHERIC RESEARCH INSTRUMENT (HAARP IRI)

V. Eccles
R. Armstrong

Mission Research Corporation
One Tara Blvd
Nashua, NH 03062-2801

May 1993

Scientific Report No. 2

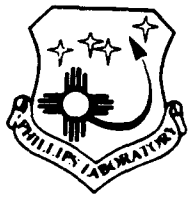

PHILLIPS LABORATORY
Directorate of Geophysics
AIR FORCE MATERIEL COMMAND
HANSCOM AIR FORCE BASE, MA 01731-3010

"This technical report has been reviewed and is approved for publication"

DONALD E. HUNTON
Contract Manager

JOHN F. PAULSON
Branch Chief

WILLIAM K. VICKERY
Division Director

This document has been reviewed by the ESD Public Affairs Office (PA) and is releasable to the National Technical Information Service (NTIS).

Qualified requestors may obtain additional copies from the Defense Technical Information Center. All others should apply to the National Technical Information Service.

If your address has changed, or if you wish to be removed from the mailing list, or if the addressee is no longer employed by your organization, please notify PL/TSI, Hanscom AFB, MA 01731-5000. This will assist us in maintaining a current mailing list.

Do not return copies of this report unless contractual obligations or notices on a specific document requires that it be returned.

REPORT DOCUMENTATION PAGE

Form Approved
OMB No. 0704-0188

1. AGENCY USE ONLY (Leave blank)	2. REPORT DATE	3. REPORT TYPE AND DATES COVERED
	May 1993	Scientific, Report No. 2

4. TITLE AND SUBTITLE
UPPER ATMOSPHERIC EFFECTS OF THE HF ACTIVE AURORAL RESEARCH PROGRAM IONOSPHERIC RESEARCH INSTRUMENT (HAARP IRI)

5. FUNDING NUMBERS
Contract F19628-90-C-0118
PE 61102F
PR 2310
TA G3 WU BM

6. AUTHOR(S)
V. Eccles and R. Armstrong

7. PERFORMING ORGANIZATION NAME(S) AND ADDRESS(ES)
Mission Research Corporation
One Tara Blvd.
Suite 302
Nashua, NH 03062-2801

8. PERFORMING ORGANIZATION REPORT NUMBER

9. SPONSORING / MONITORING AGENCY NAME(S) AND ADDRESS(ES)
Phillips Laboratory (GPIA)
29 Randolph Road
Hanscom AFB, MA 01731-3010
Contract Manager: Donald Hunton/GPID

10. SPONSORING / MONITORING AGENCY REPORT NUMBER
PL-TR-93-2150

11. SUPPLEMENTARY NOTES

12a. DISTRIBUTION / AVAILABILITY STATEMENT
Approved for Public Release
Distribution Unlimited

12b. DISTRIBUTION CODE

13. ABSTRACT *(Maximum 200 words)*

The earth's ozone layer occurs in the stratosphere, primarily between 10 and 30 miles altitude. The amount of ozone, O , present is the result of a balance between production and destruction processes. Experiments have shown that natural processes such as auroras create molecules that destroy O . One family of such molecules is called "odd nitrogen" of which nitric oxide (NO) is an example. Because the HAARP (HF Active Auroral Research Program) facility is designed to mimic and investigate certain natural processes, a study of possible effects of HAARP on the ozone layer was conducted. The study used a detailed model of the thermal and chemical effects of the high power HF beam, which interacts with free electrons in the upper atmosphere above 50 miles altitude. It was found only a small fraction of the beam energy goes into the production of odd nitrogen molecules, whereas odd nitrogen is efficiently produced by auroras. Since the total energy emitted by HAARP in the year is some 200,000 times less than the energy deposited in the upper atmosphere by auroras, the study demonstrates that HAARP HF beam experiments will cause no measurable depletion of the earth's ozone layer.

14. SUBJECT TERMS	15. NUMBER OF PAGES
Ozone Ozone Depletion Ozone Layer Odd Nitrogen Nitric Oxide HAARP Emitter Characteristics	20
	16. PRICE CODE

17. SECURITY CLASSIFICATION OF REPORT	18 SECURITY CLASSIFICATION OF THIS PAGE	19. SECURITY CLASSIFICATION OF ABSTRACT	20. LIMITATION OF ABSTRACT
UNCLASSIFIED	UNCLAS	UNCLAS	SAR

CONTENTS

INTRODUCTION	1
ODD NITROGEN-OZONE CHEMISTRY	1
MODEL OF THERMAL AND CHEMICAL EFFECTS WITHIN AN HF HEATER BEAM	5
BEAM DEPOSIT IN AN UNDERDENSE IONOSPHERE	6
RESULTS OF HF HEATING MODEL	8
DETAILED CHEMISTRY OF A PARCEL OF AIR IN AN HF BEAM	10
CONCLUSION	12
References	12

FIGURES

1.	Electron Density Profiles in and Out of the Auroral Oval	8
2.	Results of Deposition Model are for Beam Frequencies of 2.8 and 8 MHz	9
3.	(a) Energy Deposition Rates; (b) Electron Temperature Seen by a Parcle of Air Moving Through the HAARP HF Heater Beam at 30 m/s	11

TABLES

1.	Stratospheric NO Sources	4
2.	Mesospheric and Thermospheric NO Sources	4
3.	HAARP Specifications	5
4.	Electronically Excited Species Contained in the Deposition Model	7

UPPER ATMOSPHERIC EFFECTS OF THE HF ACTIVE AURORAL RESEARCH PROGRAM IONOSPHERIC RESEARCH INSTRUMENT (HAARP IRI)

SUMMARY

The ozone layer, which protects life on earth from ultraviolet rays, is contained primarily between 10 and 30 miles altitude. The amount of ozone, O_3, present in the stratosphere is a result of a balance of processes that produce ozone and processes that destroy ozone. This region of the atmosphere is called the stratosphere. Experiments have shown that natural processes, such as auroras, produce molecules that destroy ozone. One family of these molecules is called odd nitrogen. Nitric oxide (NO) belongs to this family.

Because the HAARP (HF Active Auroral Research Program) facility is designed to mimic and investigate certain natural processes, a study of the possible effects of HAARP on the ozone layer was conducted. The study used a detailed model of the thermal and chemical effects of the HF radar beam.

The HAARP facility heats the free electrons in the upper atmosphere above 50 miles altitude. Most of the heating will produce airglow and winds. Airglow is light emitted by excited air molecules. Only a small fraction of the beam energy goes to producing odd nitrogen molecules. The total energy emitted by HAARP in a year is 200,000 times less than the energy deposited in the upper atmosphere by auroras. Odd nitrogen is efficiently produced by auroras in contrast to production from processes induced by the HF beam. The comparison of the HAARP effects to natural processes in the upper atmosphere demonstrate that HAARP HF beam experiments will have no measurable depletion effects on the earth's ozone layer.

INTRODUCTION

Ambient and perturbed ionospheric conditions can be studied with HF (high-frequency) radars and cooperative experimental observations. Electron gas heating occurs in the ionosphere as the HF radar beam energy is attenuated by the atmosphere. Studying the region within the beam can give insight into hydrodynamics, chemistry, and thermal relaxation properties of the upper atmosphere. The most easily observed result of the HF induced chemistry is the enhanced airglow signatures along the magnetic field lines intersecting the HF beam.

The region of energy deposition from the HF beam can range from 50 km altitude to the F peak of the ionosphere (near 300 km). This is the same region where many natural processes deposit energy; Solar EUV and UV flux, auroral particle precipitation, joule heating in electrojet regions, solar proton events (SPE), relativistic electron precipitation (REP) and meteor showers. The energy drives important chemical reactions, which determine the chemical composition of the upper atmosphere.

Recent attention has been given to the effect of the energetic particle events on ozone layer concentration [*Jackman et al.*, 1980; *Rusch et al.*, 1981; *Orsini and Frederick*, 1982; *Frederick and Orsini*, 1982; *Solomon et al.*, 1982; *Callis et al.*, 1991]. The energetic particles ionize air molecules. The ionization and recombination chemistry produces odd nitrogen species. Important odd nitrogen species are N, NO, NO_2, NO_3, HNO_3, HNO_4. It was determined by *Crutzen* [1970] and *Johnston* [1971] that odd nitrogen plays a role in determining ozone [O_3] densities within the stratosphere and mesosphere. The amount of ozone present in the stratosphere is a result of a balance between processes that produce ozone and processes that destroy ozone. The previously cited references explored the effect of naturally produced odd nitrogen upon stratospheric ozone.

Because the HAARP facility is designed to mimic and investigate some of these natural processes, a study of the possible effects of HAARP on the ozone layer has been done. The purpose of this study is to assess the magnitude of the HAARP facility impact on the natural chemical system of the upper atmosphere. We have examined energy deposition, ionization, and odd nitrogen production within the HAARP HF beam for a year of nominal HAARP operations. The total production rates are then compared to natural sources of odd nitrogen to determine relative impact on the ozone layer.

The result of the study shows that the HAARP facility impact on the ozone layer is negligible and probably not measurable. This is demonstrated by the comparison of worst case estimates of HAARP facility impact to naturally occurring auroral effects.

ODD NITROGEN-OZONE CHEMISTRY

The ozone destruction ability of CFCs (Chloroflourocarbons) has been well publicized. Humankind can, and possibly has, globally altered the chemical composition of the atmosphere. Less known to the public is the ability of odd nitrogen molecules to destroy ozone. A network of ground based stations observed a 5% increase in the monthly mean total ozone measurement from 1960 to 1970. The increase was attributed to the return of natural ozone levels after a suppression of ozone caused by atmospheric

testing of nuclear bombs during 1961 and 1962. The nuclear tests produced 10^{34} molecules of odd nitrogen, which participated in catalytic destruction of ozone.

Ozone is primarily created through the three-body association reaction:

$$O + O_2 + M \longrightarrow O_3 + M \qquad (r1)$$

Atomic oxygen is created through photodissociation of O_2 by solar EUV in the upper atmosphere. Two important reactions of odd nitrogen destruction of ozone are:

$$NO + O_3 \longrightarrow NO_2 + O_2 \qquad (r2)$$

$$NO_2 + O \longrightarrow NO + O_2 \qquad (r3)$$

Reactions (r2) and (r3) have a combined net result of:

$$O_3 + O \longrightarrow 2O_2 \qquad \text{(net reaction)}$$

Reaction (r2) destroys ozone. The resulting NO_2 destroys atomic oxygen through reaction (r3). The loss of atomic oxygen reduces the effectiveness of (r1). The odd nitrogen molecules are not destroyed in the reactions (r2) and (r3). NO and NO_2 can participate in O_3 and O destruction repeatedly. This is the nature of a catalytic reaction. The above chemistry is simplified but demonstrates the main effect of increased odd nitrogen levels in the stratospheric ozone layer.

The chemistry used in this study is a comprehensive set of reactions [*Kennealy et al.*, 1989; Larkin, personal communication] for the regions of the HF radar energy deposition.

The largest source of odd nitrogen in the upper atmosphere is through the reaction

$$N_2O + O(^1D) \longrightarrow NO + NO \qquad (r4)$$

This source of NO produces roughly 4.5×10^{34} NO molecules per year in the stratosphere and mesosphere. High-energy particle events are important sources of odd nitrogen molecules. Energetic particles generated in solar flares produce "particle events" in the upper atmosphere. The fast protons in solar proton events (SPE) strike the atmosphere and produce an electron-ion pair. For every 35 eV of energy deposited in the atmosphere one electron-ion pair is produced. Other energetic particle events, such as relativistic electron precipitation (REP), and galactic cosmic rays (GCR), ionize air with the same efficiency. The electron impact ionizations of air are primarily

$$N_2 + e \longrightarrow N_2^+ + e + e \qquad (r5)$$

$$N_2 + e \longrightarrow N^+ + N + e + e \qquad (r6)$$

$$O_2 + e \longrightarrow O_2^+ + e + e \qquad (r7)$$

$$O_2 + e \longrightarrow O^+ + O + e + e \qquad (r8)$$

$$O + e \longrightarrow O^+ + e + e \qquad (r9)$$

Ionization of air by electron or proton impact eventually produces odd nitrogen species through recombination of an ion-electron pair.

$$NO^+ + e \longrightarrow N(^2D) + O \qquad (r10)$$

$$N_2^+ + e \longrightarrow N(^2D) + N \qquad (r11)$$

and NO production through

$$N(^2D) + O_2 \longrightarrow NO + O \qquad (r12)$$

Careful accounting of odd nitrogen production suggests that 1.3 to 1.6 odd nitrogen molecules are produced per ionization [*Rusch et al.*, 1981]. The number used most often in the literature is about 1.3. Additional sources of odd nitrogen are; ionization of air by meteors and photochemical production in the thermosphere. Solar energy deposition above 100 km altitude in the thermosphere causes ionizations and dissociations that produce NO, $N(^4S)$, and $N(^2D)$. The long-lived NO and $N(^4S)$ are subject to vertical transport. The odd nitrogen produced above 100 km altitude is transported downward to mesospheric (50-80 km) and possibly stratospheric (15-50 km) altitudes [*Solomon et al.*, 1982]. Odd nitrogen molecules, which are created above 100 km and survive the transport to the lower mesosphere and stratosphere, can participate in ozone destruction.

The only loss mechanism for NO and N during the downward transport to the stratosphere is the photodissociation of NO, coupled with a cannibalistic reaction of NO and N

$$NO + h\nu \longrightarrow N + O \qquad (r13)$$

$$N + NO \longrightarrow N_2 + O \qquad (r14)$$

The photodissociation is needed to maintain N densities because N also reacts with O_2 to produce NO (reaction (r12)).

During the long dark winters of the polar atmosphere the loss rate of odd nitrogen is very small. The probability that NO reaches the stratosphere increases. Also, the vertical motion is generally downward in the upper atmosphere through the winter season. *Solomon and others* [1982] examine high latitude odd nitrogen production and transport. They conclude that auroral activity during winter months can affect on stratospheric odd nitrogen levels. They also conclude that summer hemisphere odd nitrogen densities in the stratosphere are not appreciably enhanced by auroral activity, because the N and NO densities are brought into equilibrium through photodissociation and subsequent mutual destruction during downward transport. These conclusions are supported by reports of enhanced NO densities in the winter polar region [*Rusch and Barth*, 1975].

A comparison of natural odd nitrogen sources with the nuclear test series odd nitrogen production provides necessary context in understanding the magnitude of possible human-made perturbations. *Jackman and others* [1980] compile a list of the annual production of odd nitrogen from various sources. Table 1 and 2 contain the results of the compilation. The nuclear tests produced nearly as much odd nitrogen as the largest natural source. The tests were probably responsible for a 5% reduction of global ozone layer content.

Studies of natural odd nitrogen production in the mesosphere and thermosphere are of particular interest to the HAARP program since these are the regions of the largest energy deposition of the HF beam. The higher altitude sources can be compared to HAARP effects to ascertain HAARP impact on the ozone layer.

Table 1. Stratospheric NO sources [*Jackman et al.*, 1980].

Source	NO molecules/yr solar maximum	NO molecules/yr solar minimum
$N_2O+O(^1D)$	4.5×10^{34}	4.5×10^{34}
REPs	2.7×10^{31}	2.7×10^{30}
SPEs	2.5×10^{33}	2.5×10^{33}
GCRs	2.7×10^{33}	3.7×10^{33}
Nuclear testing 1961-62	2.2×10^{34}	2.2×10^{34}
Total without Nuclear tests	5.0×10^{34}	5.0×10^{34}

Table 2. Mesospheric and thermospheric NO sources [*Jackman et al.*, 1980].

Source	NO molecules/yr solar maximum	NO molecules/yr solar minimum
$N_2O+O(^1D)$	5.3×10^{32}	5.3×10^{32}
REPs	1.4×10^{34}	1.4×10^{33}
SPEs	3.9×10^{33}	3.9×10^{33}
Thermospheric	1.5×10^{34}	3.7×10^{33}
Meteors	6.3×10^{32}	6.2×10^{32}
Total	3.4×10^{34}	1.0×10^{34}

MODEL OF THERMAL AND CHEMICAL EFFECTS WITHIN AN HF HEATER BEAM

There are presently two mechanisms for the conversion of HF field energy to particle energy; ohmic and anomalous. In an underdense ionosphere (that is, the HF emission frequency is much less than the plasma frequency) the absorption of the HF beam takes place through ohmic heating. Beam energy is absorbed as accelerating electrons collide with ions and neutral constituents. The collisionally thermalized electrons of the E and D region are heated rapidly. On a much slower time scale, the ions and neutrals are heated through elastic and inelastic collisions with the electrons. Additionally, anomalous heating occurs when the plasma frequency approaches the HF emission frequency. Anomalous heating results from time-varying plasma instabilities and occurs in a very narrow altitude range.

HAARP specifications are listed in Table 3. Ambient backgrounds for winter nighttime are used for the investigations. The HAARP experiments to be conducted will vary in power and duty cycle. Also, some of the beam energy is not absorbed in the atmosphere, but escapes to space or reflects to the ground. Therefore, the yearly emission estimate in Table 3 can be considered an upper limit for energy deposition from the HAARP program. Experiments are to occur during all local times and seasons. Additionally, the HAARP facility will be able to illuminate regions inside and outside the active auroral region.

Table 3. HAARP specifications.

Total Beam Power	3MW ($2x10^{25}$ eV/s)
Beam width	10^o to 3^o
Effective Beam Power	0.7 to 3GW
Frequency Range	10 to 2.8 MHz
Yearly operation	320 hrs ($1.15x10^6$ s)
Operation periods	Campaigns spread evenly through seasons
Yearly emission	$3.5x10^{12}$ W/year ($2x10^{31}$ eV/year)

The total emission of a nominal HAARP campaign can be compared to the global energy budget to determine relative impact to upper atmosphere energy inputs. This is a slightly different but related question to chemical impact. Total solar, chemical, and mechanical energy input into the atmosphere is approximately $6x10^{38}$ eV/yr and $4x10^{38}$ eV/yr for solar maximum and solar minimum, respectively [*Roble et al.*,1987]. The natural energy input for a year is at least 20 million times greater than HAARP yearly emission.

As previously mentioned, the polar upper atmosphere is particularly sensitive to odd nitrogen production in the dark winter months. Due to the sensitivity of the nighttime winter atmosphere to odd nitrogen enhancements, we focus on winter ionospheric profiles. Ambient conditions were obtained from MSIS90 neutral atmosphere [*Hedin*,

1990], the E region model of *Rasmussen and others* [1989]. Electron profiles of *Ogawa and Shimazaki* [1975] are used below 90 km. The geophysical parameters of average solar activity and moderate magnetic storm activity are used in obtaining the neutral atmospheric and ionospheric profiles.

Beam Deposit in an Underdense Ionosphere

Ohmic heating of the electron gas is the assumed heating mechanism for energy deposition in the D and E region of the ionosphere. The literature has many examples of deposition calculations [*Farley*, 1963; *Thomson*, 1970; *Meltz and LeLevier*, 1970; *Showen and Behnke*, 1978; *Perkins and Roble*, 1979; *Mantas et al.*, 1981]. The approach of *Perkins and Roble* [1979] is followed and extended for the calculations presented here. For the polar ionosphere the electron energy equation can be expressed as

$$\frac{d}{dt}\left(\frac{3}{2}n_e K T_e\right) - \frac{d}{dz}\left(\lambda_e \frac{dT_e}{dz}\right) = Q_{HF} - L_{el} - L_{inel} - L_{ion} \qquad (1)$$

where t is time, z is altitude, n_e is electron density, K is Boltzmann's constant, T_e is electron temperature, u_e is electron velocity, λ_e is thermal conductivity, Q_{HF} is the HF energy deposition term, L_{el} represents all elastic collisional energy losses, L_{inel} represents all inelastic collisional energy losses, and L_{ion} represents all ionizing collisional energy losses. The ohmic HF heating term is:

$$Q_{HF} = \frac{F}{c}\left(\frac{\nu_p^2}{\nu_b^2 + \nu_e^2}\right)\nu_e \qquad (2)$$

where F is the energy flux of the beam, c is velocity of light, ν_p is the plasma frequency, ν_b is the beam frequency, and ν_e is the total electron collision frequency (that is, combined electron-neutral collision frequency, ν_{en}, and electron-ion collision frequency, ν_{ei}). The energy flux, F, is attenuated with altitude as beam energy is absorbed. A kilometer below the altitude where ν_b approaches ν_p significant energy deposition occurs due to anomalous heating. The anomalous heating can produce non-thermal electrons with energies of 2 to 10 eV [see, *Bernhardt and others* [1989] and references therein]. The anomalous heating within the HF beam is observed in the F region. A large percentage of the beam energy is absorbed in the D and E region where ohmic heating will dominate.

The heated electron gas is cooled through the transfer of energy to the heavy particle by elastic and inelastic collisions. The elastic collisional heat loss is written

$$L_{el} = \sum_i n_e \frac{m_e}{m_i}\nu_{ei} 3K(T_e - T_i) + \sum_n n_e \frac{m_e}{m_n}\nu_{en} 3K(T_e - T_n) \qquad (3)$$

Inelastic heating is considerably more complex. *Perkins and Roble* [1979] include excitation of rotational and vibrational modes of O_2 and N_2, fine structure levels of O, and the metastable species $O(^1D)$. The vibrational and rotational energy of O_2 and N_2 is quickly transferred to the efficient radiating molecules CO_2 and NO. Electronically excited molecules will radiate or be collisionally quenched.

Perkins and Roble [1979] noted that the collisional cooling of the electron gas is not sufficient to keep the electron temperature from "running away" from the neutral temperature. The "run-away" electron temperature is capped at higher energies through inelastic collisions that have larger energy loss per collision (i.e., impact excitation of higher electronic states and impact ionization). Because the HAARP radiating power is greater than those used in the *Perkins and Roble* [1979] calculation, additional excited states are included in the inelastic loss term. An impact-ionization cooling term is also added. The vibrational and rotational loss rates of *Schunk and Nagy* [1978] are used. The excited states included in the model are listed in Table 4. The electron impact excitation cross sections were obtained from *Banks and Kockarts* [1973]. The energy loss terms for inelastic collisional heat loss can be written in the form

$$L_{inel} = E_{inel} k_{inel} n_e n_n \tag{4}$$

where E_{nl} is the energy of the excitation, k_{nl} is the rate of the excitation, and n_n is the density of the neutral species.

In the beams of smaller power the E region plasma density increases due to the decrease in ion-electron recombination rates. As the electron energies increase with the increase in beam power, impact ionization may become important in determining plasma densities. The electron impact ionization cross sections were obtained from *Banks and Kockarts* [1973]. The loss terms for impact ionization have the form

$$L_{ion} = E_{IP} \alpha_n n_e n_n \tag{5}$$

where E_{IP} is the ionization potential and a_{en} is the impact ionization rate.

Table 4. Electronically excited species contained in the deposition model.

Gas	State	Energy (eV)	Lifetime (s)
N2	$A^3\Sigma_u^+$	6.14	1.9
	$B^3\Pi_g$	7.30	8.9×10^{-6}
	$C^3\Pi_u$	11.03	3.6×10^{-6}
	$a^1\Pi_g$	9.10	1.5×10^{-4}
	$b^1\Pi_u$	12.85	10^{-7}
O2	$a^1\Delta_g$	.98	3880
	$b^1\Sigma_g$	1.64	11.8
	$A^3\Sigma_u^+$	4.5	10^{-7}
	$B^3\Sigma_u^-$	8.3	10^{-7}
O	^1D	1.96	148
	^1S	4.17	.8
	^3S	9.53	1.8×10^{9}
	^5S	9.15	6×10^{-4}

Results of HF Heating Model

The two electron density profiles are used in the modeling the HAARP HF heating effects (Figure 1). Both are from polar winter. This choice is due to the sensitivity of the winter atmosphere to odd nitrogen production. For simplicity the initial electron temperature was set equal to the neutral temperature at all altitudes. The energy deposition model described in previous sections calculates magnitudes of energy deposition, electron temperature and cooling terms for HF heater beams. The HAARP program specifications call for emission of 3MW within a 3° beam width giving an effective radiative power of 3GW. Frequencies of 2.8 to 8 MHz are available to the HAARP radar. These extremes are used in the case studies presented below.

Energy deposition, beam flux, electron temperature, and ionization rates for the two electron density profiles are shown in Figure 2. The energy deposition drops off sharply below 75 km for all cases due to the lack of electrons below this altitude. The electrons attach to molecules readily through three-body attachment. During the daylight, photodetachment increases the electron density below 75 down to 60 km altitude. However, beam attenuation below 75 km during the daylight will be minimized as electron attachment is accelerated by the elevated electron temperature in the HF beam. When the beam is on, the free electron density within the beam will be reduced below 75 km altitude. Three-body attachment is not important above 85 km.

The denser ionosphere within the auroral oval reflects the 2.8 MHz beam so the flux drops to zero (Figure 2*c*). Greater energy deposition rates occur in the ionosphere of the auroral region. The beam attenuation is obvious in all examples except the 8MHz beam in the less dense ionosphere (Figure 2*c,d*).

Electron temperatures of the D and E regions calculated from the balance of cooling and heating terms are larger than the temperature enhancements calculated in the *Perkins and Roble* [1979] model of Arecibo HF heating experiments. The same total emission energy was used (3MW) but the beam width is narrower for the HAARP facility providing for larger energy fluxes.

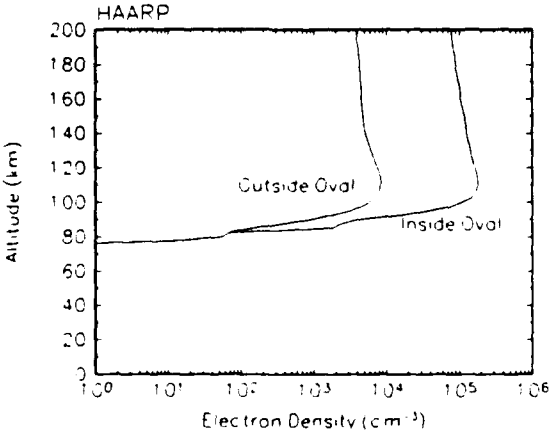

Figure 1. Electron density profiles in and out of the auroral oval. The conditions are for nighttime winter with moderate auroral activity.

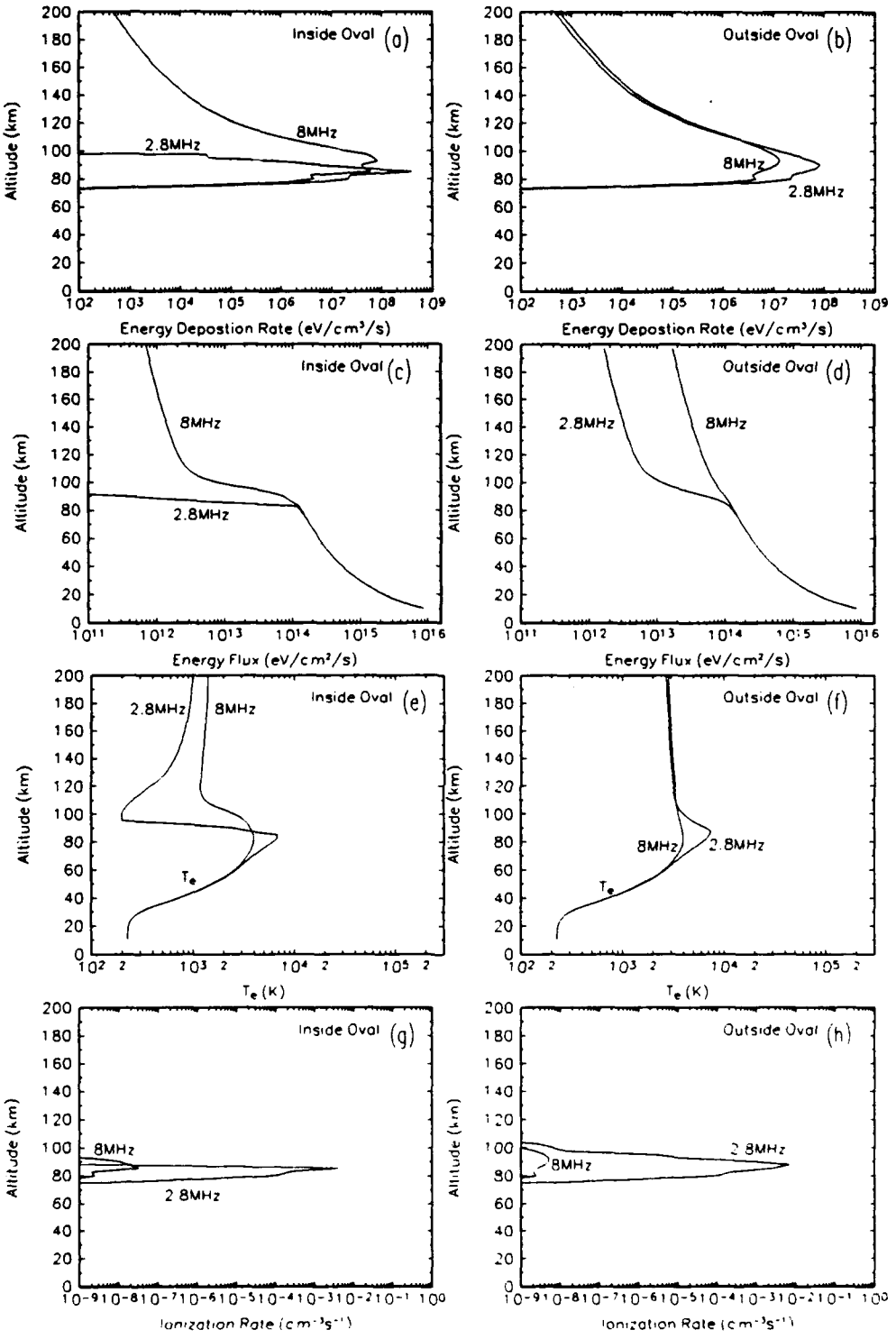

Figure 2. Results of deposition model are for beam frequencies of 2.8 and 8 MHz. Local energy deposition for (a) inside the auroral region and (b) outside the auroral region. Energy flux of HF beams for (c) inside the auroral region and (d) outside the auroral region. Electron temperatures for (e) inside auroral region and (f) outside auroral region. Ionization profiles for (g) inside the aurora zone and (h) outside the aurora zone.

A very high electron temperature results in ionization and dissociation of the neutral atmosphere through electron impact. The temperatures of .8eV at 90 km within HF beam are still not high enough for ionization or dissociation to become important. Even though the local energy deposition of the HF beam is comparable to an intense aurora, the heated electrons do ionize efficiently (Figure 4*g,h*). Most of the energy goes into vibrational and rotational excitation of O_2 and N_2. The ratio of the rates of ionization to energy deposition determined from the energy deposition model predicts one ion-electron pair produced per 10^{10} eV energy deposited. The energy deposition from high-energy particle events (>500 eV), such as in auroras, SPEs, GCEs, RPEs, produces ion-electron pairs efficiently. For such events one ion-electron pair is created per 35 eV deposited.

The impact of HF heating on the odd nitrogen chemistry can be estimated from the ion-electron pairs produced within the beam. Using the number of 1.3 odd nitrogen molecules per ion-electron pair, the total beam emission rate and 10^{10} eV per ion-electron pair, $2x10^{15}$ molecules/s are produced in the beam. We can now compare these rates to the natural production mechanisms of odd nitrogen listed in Tables 1 and 2. For the planned operation of HAARP (Table 3) an annual operation time of 10^6 s is expected. Therefore, $2x10^{21}$ odd nitrogen molecules could be produced during a year of HAARP operation. This is 14 orders of magnitude less than natural processes (Table 1 and 2).

The possibility anomalous heating within the HF beam was mention previously. Anomalous heating can produce electrons with 2 to 10 eV energy within the F region of the ionosphere. This F region heating is only a limited percentage of the beam energy. Much of the beam energy will be deposited in the D and E region where ohmic heating dominates. The higher energy electrons of anomalous heating are still less efficient in ionizing air than particle precipiation events. The ratio of one ion-electron pair per 35 eV is used for particle energies above 500 eV [*Banks and Kocharts*, 1973]. However, even if this ratio is used for the entire yearly HAARP emission, this overestimate of HAARP production of odd nitrogen would still be 5 orders of magnitude less than the natural production. These comparisons suggest that HAARP operations will have no measurable impact on the natural, global, odd nitrogen levels.

DETAILED CHEMISTRY OF A PARCEL OF AIR IN AN HF BEAM

The time-dependent detailed chemistry of a parcel of air within the HF beam can be studied using information obtained from the energy deposition model described in the previous sections. The detailed chemistry model is used to examine the efficiency of odd nitrogen molecule creation within an HF heater beam. The energy deposited within the HF beam will not produce ion-electron pairs. However, other reactions could be driven by the elevated electron temperatures. Are there other avenues of odd nitrogen production within the beam? This is the question to be answered in this section.

The calculated results of the energy deposition model of the HF beam are used to drive the chemistry of a Lagrangian parcel of air moving through the beam. At 90 km the HF beam, where the deposition peaks, is 5 km in diameter. The wind velocities vary between 0 and 60 m/s with 35 m/s average at 90 km altitude. The electron temperature and energy deposition histories for the Lagrangian parcel are shown in Figure 3. The initial densities for the detailed chemistry study are obtained from MSIS90 [*Hedin*, 1991]

and MODTRAN [*Anderson et al.*, 1986] neutral atmosphere models. Ionospheric constituents and ionization source terms were obtained from the *Rasmussen and others* [1989]. The ionospheric profile outside the auroral region is used (Figure 1). A fully time-dependent chemistry model and an extensive reaction database were used to solve a system of ordinary differential equations for 152 atmospheric species and 1844 reactions. The conditions in the air parcel are allowed to arrive at steady state before the energy deposition is increased. Two cases are studied. The first case represents a high-energy particle precipitation event that varies in time and the second case represents energy deposition in a moving parcel of air within an HF heater beam. The energy deposition profile is the same for both cases (Figure 3*a*). Only the ionization efficiencies are different.

For the first case of the high-energy particle precipitation, the energy deposition curve of 3*a* is used to drive ionization reactions whose rates are defined by the "magic number", 35 eV per one ion-electron pair. The resulting chemical changes during the high-energy particle precipitation event are plotted in Figure 4 with dotted lines. The increase in plasma density is large during the precipitation event but the plasma relaxes to previous densities with some differences in the pre- and post-event composition (that is, less O_2^+ after the event). The odd nitrogen species, NO, N, and NO_2, all increase dramatically. Only N decreases after the event. The loss of N is through reactions (r12) and (r14). NO and NO_2 remain at the elevated densities due to the lack of destruction processes during polar winter.

The second case examined was a parcel of air moving through the HF beam at 30 m/s. The electron temperature curve in Figure 3*a* was used to drive the chemistry. The electron temperature history (Figure 3*b*) was derived from the energy deposition curve show in Figure 3*a*. The neutral and ion temperature histories were also included in the model. Both temperatures only increase about 1° K during the parcel transit of the beam.

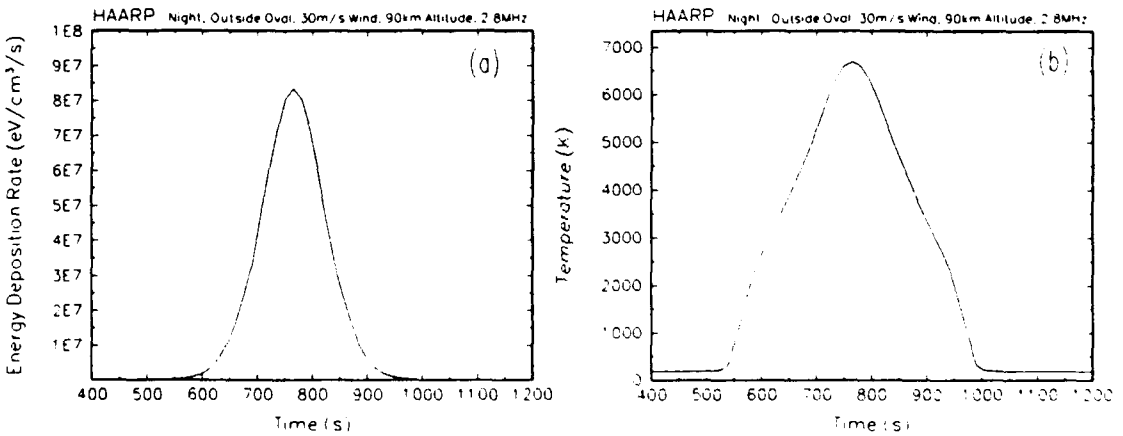

Figure 3. (a) Energy deposition rates and (b) electron temperature seen by a parcel of air moving through the HAARP HF heater beam at 30 m/s. These values are used to drive a detailed chemistry model, first, within an HF heater beam and, second, during a high-energy particle precipitation event.

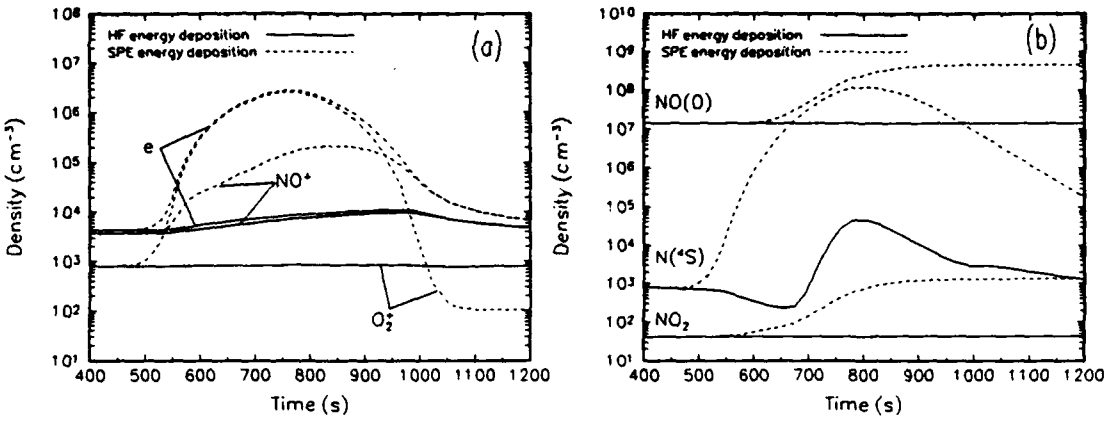

Figure 4. The chemical changes are shown for two different cases. The energy deposition is the same in both cases but one case represents HF heating effects (solid lines) and the other represents high-energy particle precipitation effects (dotted lines). (a) The main plasma constituents and (b) the odd nitrogen molecules within the air parcel are shown for the two cases.

Within the HF beam, the elevated electron temperature slowed the dissociative recombination rates. This increased the plasma density (Figure 4*a*). The increase in plasma density was not due to increased ionization levels. After leaving the beam the plasma within the parcel returns to ambient density and composition. The odd nitrogen levels are unchanged throughout the transit of the beam (Figure 4*b*). There are some constituency changes when the parcel is in the beam, such as increased metastable species, but these return to ambient levels upon beam exit or turn off. There is no observable odd nitrogen production.

CONCLUSION

The total energy emitted yearly by the HAARP facility is many orders of magnitude smaller than the mesospheric and thermospheric energy deposition by natural processes. Auroral energy deposition, which leads to ionization and odd nitrogen production, is also orders of magnitude larger than the yearly energy emission of the HAARP facility. The HAARP program will have negligible effect on the thermal and chemical structure of the global upper atmosphere.

The small region within the HF heater beam has local energy deposition rates that are comparable to intense auroras. However, this study demonstrates the inefficiencies of the HF heated electrons in producing odd nitrogen molecules.

The HAARP program will (1) not alter the natural levels of odd nitrogen in the polar upper atmosphere and (2) will have no negative impact on the ozone layer of the earth.

REFERENCES

Anderson, G.P., J.H. Chetwynd, S.A. Clough, E.P. Shettle, and F.X. Kneizys, *AFGL Atmospheric Constituent Profiles (0-120km)*, AFGL-TR-86-0110, Air Force Geophysics Laboratory, 1986. ADA175173

Banks, P.M. and G. Kockarts, *Aeronomy, Part A and B*, Academic Press, New York, 1973.

Bernhardt, P.A., C.A. Tepley, and L.M. Duncan, Airglow enhancements associated with plasma cavities formed during ionospheric heating experiments, *J. Geophys. Res., 94*, 9071-9092, 1989.

Callis, L.B., D.N. Baker, J.B. Blake, J.D. Lambeth, R.E. Boughner, M. Natarajan, R.W. Klebesadel, and D.J. Gorney, Precipitating relativistic electrons: Their long-term effect on stratospheric odd nitrogen levels, *J. Geophys. Res., 96*, 2939, 1991.

Crutzen, P.J., The influence of nitrogen oxides on the atmospheric ozone content, *Q. J. R. Meteorol. Soc.*, *96*, 320, 1970.

Farley, D.T., Artificial heating of the electrons in the F region of the ionosphere, *J. Geophys. Res., 68*, 401, 1963.

Frederick, J.E., and N. Orsini, The distribution and variability of mesospheric ode nitrogen: a theoretical investigation, *J. Atmos. Terr. Phys., 44*, 479, 1982.

Hedin, A.E., Neutral atmosphere empirical model from the surface to lower exosphere MSISE90, *J. Geophys. Res., 96*, 1159-1172, 1991.

Jackman, C.H., J.E. Frederick, and R.S. Stolarski, Production of odd nitrogen in the stratosphere and mesosphere: An intercomparison of source strengths, *J. Geophys. Res.*, 85, 7495, 1980.

Johnston, H.S. Reduction of stratospheric ozone by nitrogen oxide catalysts from SST exhaust, *Science, 173*, 517, 1971.

Kennealy, J.P., S.B. Downer, R.J. Larkin, T.J. Moratz, ARCHON-22, MRC Technical Report, 1989.

Mantas, G.P., H.C. Carlson, C. H. LaHoz, Thermal response of the F region ionosphere in artificial modification experiments by HF radio waves, *J. Geophys. Res., 86*, 1981.

Meltz, G. and R.E. LeLevier, Heating the F region by derivative absorption of radio waves, *J. Geophys. Res., 75*, 6406, 1970.

Orsini, N. and T. Shimazaki, Diurnal variations of odd nitrogen and ionic densities in the mesosphere and lower thermosphere: Simultaneous solution of photochemical-diffusive equations, *J. Geophys. Res., 80*, 3945-3960, 1975.

Orsini, N. and J.E. Frederick, Solar disturbances and mesospheric odd nitrogen, *J. Atmos. and Terr. Phys., 44*, 489, 1982.

Perkins, F.W. and R.G. Roble, Ionospheric heating by radio waves: Predictions for Arecibo and the satellite power station, *J. Geophys. Res., 83*, 1611, 1978.

Rasmussen, C.E., R.W. Schunk, and V.B. Wickwar, A photochemical equilibrium model for ionospheric conductivity, *J. Geophys. Res., 93*, 9831, 1988.

Roble, R.G., E.C. Ridley, and R.E. Dickinson, On the global mean structure of the thermosphere, *J. Geophys. Res., 92*, 8745, 1987.

Rusch, D.W., and C.A. Barth, Satellite measurements of nitric oxide in the polar region, *J. Geophys. Res., 80*, 3719, 1975.

Rusch, D.W., J.-C. Gerard, S. Solomon, P.J. Crutzen and G.C. Reid, The effect of particle precipitation events on the neutral and ion chemistry of the middle atmosphere I. Odd nitrogen, *Planet. Space Sci., 29*, 767, 1981.

Schunk, R.W., and A.F. Nagy, Electron temperature in the F region of the ionosphere: Theory and observations, *Rev. Geophys. and Space Phys., 16*, 355, 1978.

Showen, R. L., and R. A. Behnke, The effect of HF -induced plasma instabilities on ionospheric electron temperatures, *J. Geophys. Res.*, *83*, 207, 1978.

Solomon, S., P.J. Crutzen, and R.G. Roble, Photochemical coupling between the thermosphere and the lower atmosphere 1. Odd nitrogen from 50 to 120 km, *J. Geophys. Res.*, *87*, 7206, 1982.

Thomson, J.A., Energy deposition in artificial ionospheric heating experiments, *J. Geophys. Res.*, *75*, 6446, 197